

Dataless Quadratic Neural Networks for the Maximum Independent Set Problem

Ismail Alkhouri^{1,2}, Cedric Le Denmat³, Yingjie Li⁴, Cunxi Yu⁴, Jia Liu³,
 Rongrong Wang¹, Alvaro Velasquez⁵
¹Michigan State University
²University of Michigan Ann Arbor,
³The Ohio State University,
⁴University of Maryland College Park,
⁵University of Colorado Boulder

Combinatorial Optimization (CO) addresses many important problems, including the challenging Maximum Independent Set (MIS) problem. Alongside exact and heuristic solvers, differentiable approaches have emerged, often using continuous relaxations of ReLU-based or quadratic objectives. Noting that an MIS in a graph is a Maximum Clique (MC) in its complement, we propose a new quadratic formulation for MIS by incorporating an MC term, improving convergence and exploration. We show that every maximal independent set corresponds to a local minimizer, derive conditions for the MIS size, and characterize stationary points. To solve our non-convex objective, we propose solving parallel multiple initializations using momentum-based gradient descent, complemented by an efficient MIS checking criterion derived from our theory. Therefore, we dub our method as **parallelized Clique-Informed Quadratic Optimization for MIS (pCQO-MIS)**. Our experimental results demonstrate the effectiveness of the proposed method compared to exact, heuristic, sampling, and data-centric approaches. Notably, our method avoids the out-of-distribution tuning and reliance on (un)labeled data required by data-centric methods, while achieving superior MIS sizes and competitive runtime relative to their inference time. Additionally, a key advantage of pCQO-MIS is that, unlike exact and heuristic solvers, the runtime scales only with the number of nodes in the graph, not the number of edges.

1. Introduction

In his landmark paper [1], Richard Karp established a connection between Combinatorial Optimization Problems (COPs) and the NP-hard complexity class, implying their inherent computational challenges. Additionally, Richard Karp introduced the concept of reducibility among combinatorial problems that are complete for the complexity class NP.

Although there exists a direct reduction between some COPs – such as the case with the Maximum Independent Set (MIS), Maximum Clique (MC), and Minimum Vertex Cover (MVC) – which allows a solution for one problem to be directly used to solve another, other COPs differ significantly. For example, the case of MIS and the Kidney Exchange Problem (KEP) [2] (or the Travelling Salesman Problem (TSP) [3]) where there is no straightforward reduction between these problems. In this paper, we focus on the MIS problem, one of the most fundamental in combinatorial optimization, with many applications including frequency assignment in wireless networks [4], task scheduling [5], genome sequencing [6, 7], and multi-robot coordination [8].

The MIS problem involves finding a subset of vertices in a graph $G = (V, E)$ with maximum cardinality, such that no two vertices in this subset are connected by an edge [9]. In the past few decades, in addition to commercial Integer Programming (IP) solvers (e.g., CPLEX [10], Gurobi [11], and most recently CP-SAT [12]), powerful heuristic methods (e.g., ReduMIS in [13]) have been introduced to tackle the complexities inherent in the MIS problem. Such solvers can be broadly classified

into heuristic algorithms [14], branch-and-bound-based global optimization methods [15], and approximation algorithms [16].

More recently, differentiable approaches have been explored [17]. These approaches fall into two categories: (i) data-driven methods, where a neural network (NN) is trained to fit a distribution over training graphs, and (ii) dataless methods [18, 19]. In both cases, a continuous relaxation of either the MIS Quadratic Unconstrained Binary Optimization (QUBO) or ReLU-based objective functions is employed. Data-driven approaches are known for their unsatisfactory *generalization* performance when faced with graph instances exhibiting structural characteristics different from those in the training dataset [20]. This has also been argued recently in [?]. See Appendix B for detailed discussion about related works.

In this paper, we present a new differentiable dataless solver for the MIS problem based on an improved quadratic optimization formulation, a parallel optimization strategy, and momentum-based gradient descent, which we dub as **parallelized Clique-Informed Quadratic Optimization** for the MIS problem (pCQO-MIS). The contributions of our work are summarized as follows:

1. **MIS Quadratic Formulation with MC Term:** Leveraging the direct relationship between the MIS and MC problems, we propose a novel approach that incorporates an MC term into the continuous relaxation of the MIS quadratic formulation.
2. **Theoretically:**
 - We derive sufficient and necessary condition for the parameter that penalizes the inclusion of adjacent nodes and MC term parameter w.r.t. the MIS size.
 - We show that all local minimizers are binary vectors that sit on the boundary of the box constraints, and establish that all these local minimizers correspond to maximal independent sets.
 - We prove that if non-binary stationary points exist, they are saddle points and not local minimizers, with their existence depending on the graph type and connectivity.
3. **Optimization Strategy:** To improve exploration with our non-convex optimization, we propose the use of GPU parallel processing of several initializations for each graph instance using projected momentum-based gradient descent.
4. **Efficient MIS Checking:** Drawing from our theoretical results on local minimizers and other stationary points, we develop an efficient MIS checking function that significantly accelerates our implementation.
5. **Experimental Validation:** We evaluate our approach on challenging benchmark graph datasets, demonstrating its efficacy. Our method achieves competitive or superior performance compared to state-of-the-art heuristic, exact, and data-driven approaches in terms of MIS size and/or runtime.

2. Preliminaries

Notations: Consider an undirected graph represented as $G = (V, E)$, where V is the vertex set and $E \subseteq V \times V$ is the edge set. The cardinality of a set is denoted by $|\cdot|$. The number of nodes (resp. edges) is denoted by $|V| = n$ (resp. $|E| = m$). Unless otherwise stated, for a node $v \in V$, we use $\mathcal{N}(v) = \{u \in V \mid (u, v) \in E\}$ to denote the set of its neighbors. The degree of a node $v \in V$ is denoted by $d(v) = |\mathcal{N}(v)|$, and the maximum degree of the graph by $\Delta(G)$. For a subset of nodes $U \subseteq V$, we use $G[U] = (U, E[U])$ to represent the subgraph induced by the nodes in U , where $E[U] = \{(u, v) \in E \mid u, v \in U\}$. Given a graph G , its complement is denoted by $G' = (V, E')$, where $E' = V \times V \setminus E$ is the set of all the edges between nodes that are not connected in G . Consequently, if $|E'| = m'$, then $m + m' = n(n-1)/2$ represents the number of edges in the complete graph on V . For any $v \in V$, $\mathcal{N}'(v) = \{u \in V \mid (u, v) \in E'\}$ denotes the neighbour set of v in the complement graph $G' = (V, E')$. The graph adjacency matrix of graph G is denoted by $\mathbf{A}_G \in \{0, 1\}^{n \times n}$. We use \mathbf{I} to denote the identity matrix. The element-wise product of two matrices \mathbf{A} and \mathbf{B} is denoted by $\mathbf{A} \circ \mathbf{B}$. The trace of a matrix \mathbf{A} is denoted by $\text{tr}(\mathbf{A})$. We use $\text{diag}(\mathbf{A})$ to denote the diagonal of \mathbf{A} . For any

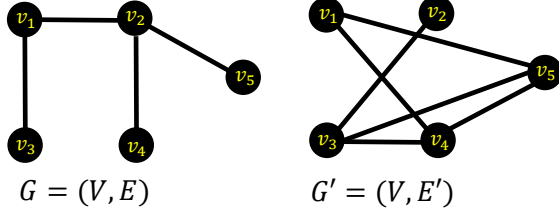


Figure 1: A graph G (left) and its complement graph G' (right): Sets $\text{MIS}_1 = \{v_1, v_4, v_5\}$ and $\text{MIS}_2 = \{v_3, v_4, v_5\}$ correspond to a maximum independent set in G and an MC in G' . Set $\text{MaxIS} = \{v_2, v_3\}$ corresponds to a maximal independent set as its not of maximum cardinality, whereas set $\text{IS} = \{v_1, v_4\}$ is an independent set as v_5 can be included in the set.

positive integer n , $[n] := \{1, \dots, n\}$. The vector (resp. matrix) of all ones and size n (resp. $n \times n$) is denoted by \mathbf{e}_n (resp. $\mathbf{J}_n = \mathbf{e}_n \mathbf{e}_n^T$). For any vector \mathbf{x} , $\mathbf{x}^T \mathbf{x} = \|\mathbf{x}\|_2^2$ and $\|\mathbf{x}\|_1^2 = \mathbf{x}^T \mathbf{J}_n \mathbf{x}$. Furthermore, we use $\mathbf{1}(\cdot)$ to denote the indicator function that returns 1 (resp. 0) when its argument is True (resp. False).

Problem Statement: In this paper, we consider the NP-hard problem of obtaining the maximum independent set (MIS). Next, we formally define MIS and the complementary Maximum Clique (MC) problems.

Definition 1 (MIS Problem). *Given an undirected graph $G = (V, E)$, the goal of MIS is to find a subset of vertices $\mathcal{I} \subseteq V$ such that $E(\mathcal{I}) = \emptyset$, and $|\mathcal{I}|$ is maximized.*

Definition 2 (MC Problem). *Given an undirected graph $G = (V, E)$, the goal of MC is to find a subset of vertices $\mathcal{C} \subseteq V$ such that $G[\mathcal{C}]$ is a complete graph, and $|\mathcal{C}|$ is maximized.*

For the MC problem, the MIS of a graph is an MC of the complement graph [1]. This means that \mathcal{I} in G is equivalent to \mathcal{C} in G' . Given a graph G , if \mathcal{I} is a Maximal Independent Set (MaxIS), then $E(\mathcal{I}) = \emptyset$, but $|\mathcal{I}|$ is not necessarily the largest in G . If \mathcal{I} is an Independent Set (IS), then $E(\mathcal{I})$ is an empty set, but there exists at least one $v \notin \mathcal{I}$ such that $E(\mathcal{I} \cup \{v\}) = \emptyset$. See Figure 1 for an example.

Let each entry of the binary vector $\mathbf{z} \in \{0, 1\}^n$ corresponds to a node $v \in V$, and is denoted by $z_v \in \{0, 1\}$. An integer linear program (ILP) for MIS can be formulated as follows [21]:

$$\max_{\mathbf{z} \in \{0,1\}^n} \sum_{v \in V} z_v \quad \text{s.t.} \quad z_v + z_u \leq 1, \forall (v, u) \in E. \quad (1)$$

The following Quadratic Unconstrained Binary Optimization (QUBO) in (2) (with an optimal solution that is equivalent to the optimal solution of the above ILP) can also be used to formulate the MIS problem [22]:

$$\max_{\mathbf{z} \in \{0,1\}^n} \mathbf{e}_n^T \mathbf{z} - \frac{\gamma_Q}{2} \mathbf{z}^T \mathbf{A}_G \mathbf{z}, \quad (2)$$

where $\gamma_Q > 0$ a parameter that penalizes the selection of two nodes with an edges connecting them. In [23], it was shown that $\gamma_Q > 1$ is sufficient and necessary condition for local minimizers to correspond to binary vectors.

3. Clique-Informed Differentiable Quadratic MIS Optimization

In this section, we first introduce our clique-Informed quadratic optimization (CQO) for the MIS problem. Then, we present theoretical insights into the objective function, followed by describing our parallelized optimization strategy with MGD.

3.1. Optimization Formulation

Our proposed optimization is

$$\min_{\mathbf{x} \in [0,1]^n} f(\mathbf{x}) := -\mathbf{e}_n^T \mathbf{x} + \frac{\gamma}{2} \mathbf{x}^T \mathbf{A}_G \mathbf{x} - \frac{\gamma'}{2} \mathbf{x}^T \mathbf{A}_{G'} \mathbf{x}, \quad (3)$$

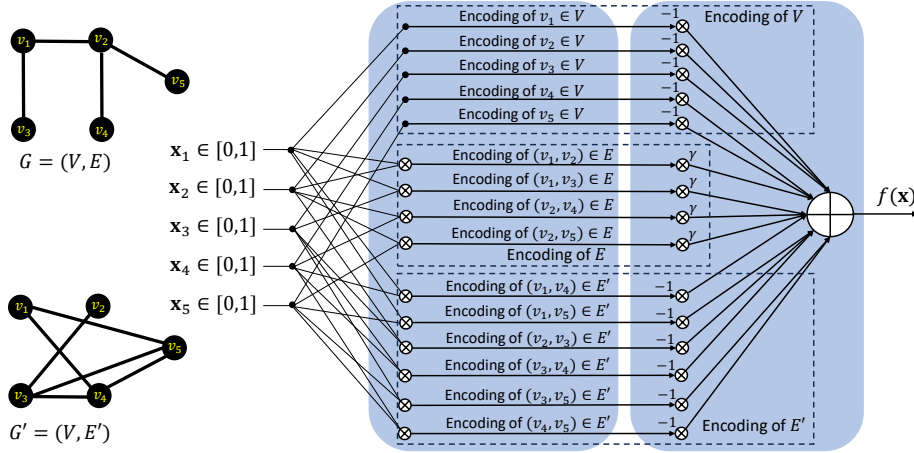


Figure 2: Graph G (left) and its corresponding dataless quadratic neural network (right).

where $\gamma > 1$, similar to γ_Q in (2), is the edges penalty parameter, and the third term is the MC term that we propose to use in this paper with parameter $\gamma' \geq 1$, introduced to discourage sparsity in the solution. Function $f(\mathbf{x})$ can also be written as

$$f(\mathbf{x}) := - \sum_{v \in V} \mathbf{x}_v + \gamma \sum_{(u,v) \in E} \mathbf{x}_v \mathbf{x}_u - \gamma' \sum_{(u,v) \in E'} \mathbf{x}_v \mathbf{x}_u .$$

Using the fact $\mathbf{A}_{G'} = \mathbf{J}_n - \mathbf{I} - \mathbf{A}_G$ in (3), our proposed function can be also rewritten as

$$f(\mathbf{x}) = -\mathbf{e}_n^T \mathbf{x} + \frac{\gamma + \gamma'}{2} \mathbf{x}^T \mathbf{A}_G \mathbf{x} + \frac{\gamma'}{2} (\|\mathbf{x}\|_2^2 - \|\mathbf{x}\|_1^2). \quad (4)$$

In particular, we incorporate the edges-penalty parameter γ that scales the influence of the edges of the graph G on the optimization objective. The third term is informed by the complementary relation between the MIS and MC problems.

The rationale behind the third term $-\frac{\gamma'}{2} \mathbf{x}^T \mathbf{A}_{G'} \mathbf{x}$ in (3) (corresponding to the edges of the complement graph G') is to (i) encourage the optimizer to select two nodes with no edge connecting them in G (implying an edge in G'), and (ii) discourage sparsity as shown in the last term of (4).

Let \mathbf{z}^* be a binary minimizer of (3) with $\mathcal{I}(\mathbf{z}^*) = \{v \in V : \mathbf{z}_v^* = 1\}$ and $|\mathcal{I}(\mathbf{z}^*)| = k$, then $f(\mathbf{z}^*) = -\sum_{v \in V} \mathbf{1}(\mathbf{z}_v^* = 1) - \gamma' |E'(\mathcal{I}(\mathbf{z}^*))|$. This includes the first and third terms only as there are not any edges connecting any two nodes in $\mathcal{I}(\mathbf{z}^*)$.

Remark 1. Given that the number of non-zero entries in \mathbf{A}_G is $2m$, then the computational cost of the QUBO formulation in (2) is $\mathcal{O}(mn)$, which is the same computational cost of our proposed function as (4) is equivalent to (3).

The proposed objective in (3) corresponds to a dataless quadratic neural networks (dQNN), illustrated in Figure 2 (right). Here, the dQNN comprises two fully connected layers. The initial activation-free layer encodes information about the nodes (top $n = 5$ connections), edges of G (middle $m = 4$ connections), and edges of G' (bottom $m' = 6$ connections), all without a bias vector. The subsequent fully connected layer is an activation-free layer performing a vector dot-product between the fixed weight vector (with -1 corresponding to the nodes and edges of G' and the edges-penalty parameter γ), and the output of the first layer.

3.2. Theoretical Insights

In this subsection, we examine the constant hessian of $f(\mathbf{x})$ in (3), and provide the necessary and sufficient condition for γ and γ' for any MIS to correspond to local minimizers of (3). Moreover, we also provide a sufficient condition for all local minimizers of (3) to be associated with a MIS. Additionally, we show the existence of a non-binary stationary point. We relegate the detailed proofs to Appendix A.

Definition 3 (MIS vector). *Given a graph $G = (V, E)$, a binary vector $\mathbf{x} \in \{0, 1\}^n$ is called a MIS vector if there exists a MIS \mathcal{I} of G such that $\mathbf{x}_i = 1$ for all $i \in \mathcal{I}$, and $\mathbf{x}_i = 0$ for all $i \notin \mathcal{I}$.*

Lemma 1. *For any non-complete graph G , the constant hessian of $f(\mathbf{x})$ in (3) is always a non-PSD matrix.*

Proof Sketch: Here, we show that the hessian is a non PSD matrix by showing that for any MIS vector \mathbf{x} , the condition $\mathbf{x}^T(\gamma \mathbf{A}_G - \gamma' \mathbf{A}_{G'})\mathbf{x} \geq 0$ is not satisfied. The result in Lemma 1 indicates that our quadratic optimization problem is always non-convex for any non-complete graph.

Theorem 1 (Necessary and Sufficient Condition on γ and γ' for MIS vectors to be local minimizers of (3)). *Given an arbitrary graph $G = (V, E)$ and its corresponding formulation in (4), suppose the size of the largest MIS of G is k . Then, $\gamma \geq \gamma'k + 1$ is necessary and sufficient for all MIS vectors to be local minimizers of (3) for arbitrary graphs.*

Proof Sketch: Given an MIS \mathcal{I} with $|\mathcal{I}| = k$, we derive the bound by considering the boundary points enforced by the box-constraints, and the gradient of $f(\mathbf{x})$ w.r.t. some $v \in V \setminus \mathcal{I}$.

Remark 2. Theorem 1 provides a guideline for choosing γ and γ' . Note that the MIS set size k is usually unknown a priori. But we may employ any classical estimate of the MIS size k to guide the choice of γ and γ' (e.g., we know from [24] that $k \geq \sum_{v \in V} \frac{1}{1+d(v)}$).

Next, we provide further characterizations of the local minimizers of (3).

Lemma 2. *All local minimizers of (3) are binary vectors.*

Proof Sketch: We prove this by showing that for any coordinates of \mathbf{x} with non-binary values, one necessary condition for any local minimizer can not be satisfied.

Building on the result of the previous lemma, we provide a stronger condition on γ and γ' that ensures all local minimizers of (4) correspond to a MIS.

Theorem 2 (Local Minimizers of (3)). *Given graph $G = (V, E)$ and set $\gamma > 1 + \gamma' \Delta(G')$, all local minimizers of (3) are MIS vectors of G .*

Proof Sketch: By Lemma 2, we examine the local minimizers that are binary. With this, we prove that all local minimizers are ISs. Then, we show that any IS, that is not maximal, is not a local minimizer.

Remark 3. The assumption $\gamma > 1 + \gamma' \Delta(G')$ in Theorem 2 is stronger than that in Theorem 1. The trade-off of choosing a large γ -value is that while larger values of γ ensure that only MIS are local minimizers, they also increase the non-convexity of the optimization problem, thereby making it more difficult to solve.

Remark 4. Although the proposed constrained quadratic Problem (3) is still NP-hard to solve for the global minimizer, it is a relaxation of the original integer programming problem. It can leverage gradient information, allowing the use of high-performance computational resources and parallel processing to enhance the efficiency and scalability of our approach.

In the following theorem, we provide results regarding points where the gradient of $f(\mathbf{x})$ is zero.

Theorem 3 (Non-Extremal Stationary Points). *For any graph G , assume that there exists a point \mathbf{x}' such that $\nabla_{\mathbf{x}} f(\mathbf{x}') = \mathbf{0}$, i.e., $\mathbf{x}' = (\gamma \mathbf{A}_G - \gamma' \mathbf{A}_{G'})^{-1} \mathbf{e}_n$. Then \mathbf{x}' is not a local minimizer of (3) and therefore does not correspond to a MIS.*

Proof Sketch: We show that its not a local minimizer by showing that it can not be binary, building upon the result on Lemma 2.

Remark 5. The above theorem suggests that while there may still exist a non-binary stationary point \mathbf{x}' , it is a *saddle point*, not a local minimizer, as indicated by the gradient being zero and by Lemma 1. Momentum-based Gradient Descent (MGD) is typically effective at escaping saddle points and converging to local minimizers, which motivates its use in pCQO-MIS. Furthermore, we observe that this specific saddle point is never encountered in our empirical evaluations and that it depends on the structure of the graph. In many cases, it lies outside the box constraints, depending on the graph's density. Further discussion is provided in Appendix C.3.

3.3. Optimization Strategy

Given the highly non-convex nature of our optimization problem, in this section, we present our pCQO-MIS method for obtaining efficient MISs¹. We first describe the projected MGD used and the parallel initializations. We then present the efficient MIS checking criterion, followed by presenting the algorithm.

3.3.1. Projected Momentum-based Gradient Descent

Our objective function in (3) is highly non-convex which makes finding the global minimizer(s) a challenging task. However, first-order gradient-based optimizers are effective for finding a local minimizer given an initialization in $[0, 1]^n$. Due to the full differentiability of our objective in (3), where the gradient vector is

$$\mathbf{g}(\mathbf{x}) := \nabla_{\mathbf{x}} f(\mathbf{x}) = -\mathbf{e}_n + (\gamma \mathbf{A}_G - \gamma' \mathbf{A}_{G'}) \mathbf{x}, \quad (5)$$

MGD empirically proves to be computationally highly efficient. Define \mathbf{v} , $\beta \in [0.5, 1)$, and $\alpha > 0$ as MGD's velocity vector, momentum parameter, and optimization step size, respectively. Then, the updates of projected MGD [?] are

$$\mathbf{v} \leftarrow \beta \mathbf{v} + \alpha \mathbf{g}(\mathbf{x}), \quad (6)$$

$$\mathbf{x} \leftarrow \text{Proj}_{[0,1]^n}(\mathbf{x} - \mathbf{v}). \quad (7)$$

We employ the updates in (6) following our empirical observation that fixed-step-size gradient descent updates for (3) is sensitive to the choice of the step size and often fail to converge to local minimizers due to overshooting. This is our rationale for adopting MGD.

3.3.2. Degree-based Parallel Initializations

For a single graph, we propose to use various points in $[0, 1]^n$ and execute the updates in (6) in parallel for each. Given a specified number of parallel processes M , we define S_{ini} to denote the set of multiple initializations, where $|S_{\text{ini}}| = M$.

Based on the intuition that vertices with higher degrees are less likely to belong to an MIS compared to those with lower degrees [18], we set S_{ini} with M samples drawn from a Gaussian distribution $\mathcal{N}(\mathbf{m}, \eta \mathbf{I})$. Here \mathbf{m} is the mean vector, initially set to \mathbf{h} as follows:

$$\mathbf{h}_v = 1 - \frac{d(v)}{\Delta(G)}, \forall v \in V, \quad \mathbf{h} \leftarrow \frac{\mathbf{h}}{\max_v \mathbf{h}_v}. \quad (8)$$

η is a hyper-parameter that governs the exploration around \mathbf{h} . After the optimization of every initialization is complete, we apply MIS checking for each, which we discuss next.

3.3.3. Efficient Implementation of MIS Checking

Given a binary vector $\mathbf{z} \in \{0, 1\}^n$ with $\mathcal{I}(\mathbf{z}) = \{v \in V : \mathbf{z}_v = 1\}$, the standard approach to check whether it is an IS and then whether it is a MaxIS involves iterating over all nodes to examine their neighbors. Specifically, this entails verifying that (i) no two nodes $(v, u) \in E$ with $\mathbf{z}_v = \mathbf{z}_u = 1$ exist (IS checking), and (ii) there does not exist any $u \notin \mathcal{I}(\mathbf{z})$ such that $\forall w \in \mathcal{I}(\mathbf{z}), u \notin \mathcal{N}(w)$ (MaxIS checking). However, as the order and density of the graph increase, the computational time required for this process may become significantly longer.

For IS checking, matrix multiplication can be used to verify whether the condition $\mathbf{z}^T \mathbf{A}_G \mathbf{z} = 0$ holds as this corresponds to the edges in the graph. If this expression results in a value strictly more than 0, then \mathbf{z} can be immediately identified as not an IS. Although this approach efficiently applies IS checking, it can not determine whether the IS is maximal.

¹The work in [25] details the complexity of box-constrained continuous non-convex quadratic optimization problems.

Algorithm 1 p-CQO-MIS.

Input: Graph $G = (V, E)$, set of initializations S_{ini} , number of iterations T per one initialization, edge-penalty parameter γ , MC term parameter γ' , and MGD parameters: Step size α , and momentum parameter β .

Output: The best obtained MaxIS \mathcal{I}^* in G

```
01: Initialize  $S_{\text{MaxIS}} = \{\cdot\}$  (Empty set to collect MaxISs)
02: For  $\mathbf{x}[0] \in S_{\text{ini}}$  (Parallel Execution)
03:   Initialize  $\mathbf{v}[0] \leftarrow \mathbf{0}$ 
04:   For  $t \in [T]$ 
05:     Obtain  $\mathbf{v}[t] = \beta\mathbf{v}[t-1] + \alpha\mathbf{g}(\mathbf{x}[t-1])$ 
06:     Obtain  $\mathbf{x}[t] = \text{Proj}_{[0,1]^n}(\mathbf{x}[t-1] - \mathbf{v}[t])$ 
07:     Obtain  $\mathbf{z}[T]$  with  $\mathbf{z}_v[T] = \mathbb{1}(\mathbf{x}_v[T] > 0), \forall v \in V$ 
08:     If  $\mathbb{1}(\mathbf{z}[T] = \text{Proj}_{[0,1]^n}(\mathbf{z}[T] - \alpha\mathbf{g}(\mathbf{z}[T])))$ 
09:       Then  $S_{\text{MaxIS}} \leftarrow S_{\text{MaxIS}} \cup \mathcal{I}(\mathbf{z}[T])$ 
10: Return  $\mathcal{I}^* = \text{argmax}_{\mathcal{I} \in S_Q} |\mathcal{I}|$ 
```

In this subsection, based on the characteristics of the local minimizers and the non-extremal stationary points of (3), discussed in Lemma 2, Theorem 2, and Theorem 3, we propose an efficient implementation to check whether a vector $\mathbf{x} \in [0, 1]^n$ corresponds to a MaxIS. In particular, in Lemma 2, we demonstrate that all local minimizers are binary. Subsequently, in Theorem 2, we establish that all local minimizers correspond to MaxISs. This implies that all binary stationary points in our box-constrained optimization in (4) are local minimizers located at the boundary of $[0, 1]^n$ and correspond to MaxISs. The latter is further elaborated upon in the proof of Theorem 2. To this end, we propose a new MaxIS checking condition that also depends on a single matrix-vector multiplication. Given some $\mathbf{x} \in [0, 1]^n$, we first obtain its binary representation as a vector \mathbf{z} , where $\mathbf{z}_v = \mathbb{1}(\mathbf{x}_v > 0)$ for all $v \in V$. Then, we propose verifying whether the following condition is satisfied.

$$\mathbb{1}(\mathbf{z} = \text{Proj}_{[0,1]^n}(\mathbf{z} - \alpha\mathbf{g}(\mathbf{z}))). \quad (9)$$

Eq. (9) is a simple projected gradient descent step to check whether \mathbf{z} is at the boundary of the box-constraints. If (9) is True, then the MaxIS is

$$\mathcal{I}(\mathbf{z}) := \{v \in V : \mathbf{z}_v = 1\} \quad (10)$$

Remark 6. As previously discussed, the work in [23] showed that any binary minimizer of a box-constrained continuous relaxation of (2) corresponds to a MaxIS when $\gamma_Q > 1$. This means that verifying whether a binary vector corresponds to a MaxIS using the proposed projected gradient descent step can also be applied using (2) as given in (11).

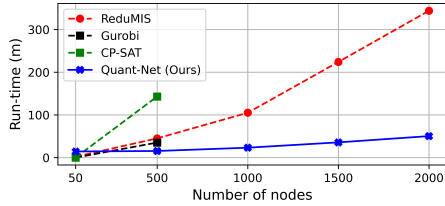
$$\mathbb{1}(\mathbf{z} = \text{Proj}_{[0,1]^n}(\mathbf{z} + \alpha\mathbf{e}_n - \frac{\alpha\gamma_Q}{2}\mathbf{A}_G\mathbf{z})). \quad (11)$$

In Section 4.4, we show the speedups obtained from using this approach as compared to the standard iterative approach discussed earlier in this subsection.

3.3.4. The pCQO-MIS Algorithm

Here, we outline the proposed procedure in Algorithm 1. As shown, the algorithm takes a graph G , the set of initializations S_{ini} , the maximum number of iterations per batch T (with iteration index t), the edge-penalty parameter γ , the MC term parameter γ' , step size α , and momentum parameter β .

For each initialization vector in set S_{ini} and iteration $t \in [T]$, Lines 5 and 6 include updating the optimization variable $\mathbf{x}[t]$. After T iterations, in Lines 7 to 9, the algorithm checks whether the binary representation of $\mathbf{x}[T]$ corresponds to a MaxIS. Finally, the best-found MaxIS, determined by its cardinality, is returned in Line 10.



(a) Total Run-time (minutes).

(n, m)	ReduMIS	Gurobi	CP-SAT	pCQO-MIS (Ours)
(50, 613)	7.6	7.6	7.6	7.6
(500, 62375)	13.4	13.4	13.4	13.4
(1000, 249750)	15	N/A	N/A	15
(1500, 562125)	16	N/A	N/A	16
(2000, 999500)	16.4	N/A	N/A	16.4

(b) Average MIS size.

Figure 3: Scalability results for the GNM graphs with $m = \lceil \frac{n(n-1)}{4} \rceil$. Each entry in the table corresponds to an average of 5 graphs. This choice of the number of edges indicates that half of the total possible edges (w.r.t. the complete graph) exist. The ‘N/A’ entries are due excessive run-times. Degree-based initializations are used here for pCQO-MIS.

After $M > 1$ optimizations is complete (i.e., when the batch is complete), set S_{ini} is constructed again, and Algorithm 1 is run again, depending on the time budget and the availability of the computational resources. The reconstruction of S_{ini} for subsequent runs is either done by sampling from $\mathcal{N}(\mathbf{h}, \eta \mathbf{I})$ (which we term by **pCQO-MIS-1**), or by setting \mathbf{m} to the optimized vector of the best obtained MaxIS from the previous run (which we term by **pCQO-MIS-2**).

4. Experimental results

4.1. Settings, Baselines, & Benchmarks

Graphs are processed using the NetworkX library [26]. For baselines, we utilize Gurobi [11] and the recent Google solver CP-SAT [12] for the ILP in (1), ReduMIS [13], iSCO² [27], and four learning-based methods: DIMES [28], DIFUSCO [29], LwD [30], and the GCN method in [31] (commonly referred to as ‘Intel’). We note that, following the analysis in [20], GCN’s code cloning to ReduMIS is disabled, which was also done in [28, 29]. To show the impact of the MC term, we include the results of pCQO-MIS without the third term (i.e., $\gamma' = 0$) which we term by pQO-MIS.

Aligned with recent SOTA methods (DIMES, DIFUSCO, and iSCO), we employ the Erdos-Renyi (ER) [32] graphs from [28] and the SATLIB graphs [33] as benchmarks. Additionally, the GNM random graph generator function of NetworkX is utilized for our scalability experiment. The ER dataset³ consists of 128 graphs with 700 to 800 nodes and $p = 0.15$, where p is the probability of edge creation. The SATLIB dataset consists of 500 graphs (with at most 1,347 nodes and 5,978 edges).

For pCQO-MIS, the parameters are set as given in Table 3 of the Appendix. Further implementation details and results are provided in Appendix C. Our code is available online⁴.

4.2. ER and SATLIB Benchmark Results

Here, we present the results of pCQO-MIS, along with the other considered baselines using the SATLIB and ER benchmarks in terms of average MIS size over the graphs in the dataset and the total sequential run-time required to obtain the results for all the graphs. Results are in Table 1. We note that the results of the learning-based methods are sourced from [28] where an A100 GPU is used.

We show pCQO-MIS results using different run-times, following the time required for ReduMIS. We note that the results of ReduMIS and exact solvers are limited to 30 seconds per graph for which an A100 GPU (with I9-12900k (hyperthreading disabled) and 32GB of DDR5 6000MHz ram) is used to report the results of all methods. In what follows, we provide observations on these results.

²<https://github.com/google-research/discs>

³<https://github.com/DIMESTeam/DIMES>

⁴<https://github.com/ledenmat/pCQO-mis-benchmark/blob/mgd/README.md>

Method	Type	Dataset: SATLIB			Dataset: ER		
		Training Data	MIS Size (\uparrow)	Run-time (\downarrow)	Training Data	MIS Size (\uparrow)	Run-time (\downarrow)
ReduMIS [13]	Heuristics	×	425.96	37.58	×	44.87	52.13
CP-SAT [12]	Exact	×	425.96	0.56	×	41.15	64
Gurobi [11]	Exact	×	425.96	8.32	×	39.14	64
GCN [31]	SL+G	SATLIB	420.66	<u>23.05</u>	SATLIB	34.86	<u>23.05</u>
LwD [34]	RL+S	SATLIB	422.22	<u>18.83</u>	ER	41.14	<u>6.33</u>
DIMES [28]	RL+TS	SATLIB	423.28	<u>20.26</u>	ER	42.06	<u>12.01</u>
DIFUSCO [29]	RL+G	SATLIB	424.5	<u>8.76</u>	ER	38.83	<u>8.8</u>
DIFUSCO [29]	RL+S	SATLIB	425.13	<u>23.74</u>	ER	41.12	<u>26.27</u>
iSCO [27]	S	×	423.7	~7500	×	44.8	~384
pQO-MIS (i.e., $\gamma' = 0$)	QO	×	412.888	16.964	×	40.398	5.78
pCQO-MIS-1	QO	×	423.184	56.399	×	45	62.93
pCQO-MIS-1	QO	×	422.384	30.129	×	44.953	40.1
pCQO-MIS-1	QO	×	421.316	21.361	×	44.85	20.11
pCQO-MIS-1	QO	×	419.476	16.976	×	44.39	5.78
pCQO-MIS-2	QO	×	424.392	51.546	×	44.56	63.23
pCQO-MIS-2	QO	×	424.3	32.017	×	44.53	41.56
pCQO-MIS-2	QO	×	423.712	20.3	×	44.45	19.89
pCQO-MIS-2	QO	×	421.594	16.394	×	44.18	6.53

Table 1: Benchmark dataset results in terms of **average MIS size** and **total sequential run-time** (minutes). RL, SL, G, QO, S, and TS represent Reinforcement Learning, Supervised Learning, Greedy decoding, Quadratic Optimization, Sampling, and Tree Search, respectively. The results of the learning-based methods (other than DIFUSCO) and ReduMIS are sourced from [28] and run using a single NVIDIA A100 40GB GPU and AMD EPYC 7713 CPU. The results of DIFUSCO are sourced from [29] and run using a single NVIDIA V100 GPU and Intel Xeon Gold 6248 CPU. The run-time for learning methods exclude the training time. The p-CQO-MIS, CP-SAT, and Gurobi results are run using an NVIDIA RTX3070 GPU and Intel I9-12900K CPU. We note that the run time reported in iSCO (Table 1 in [27]) is for running multiple graphs in parallel, not a sequential total run time. Therefore, we ran a few graphs sequentially and obtained the extrapolated run-time in row 11. ReduMIS employs the local search procedure from [35] for multiple rounds, which no other method in the table uses, following the study in [20]. For more details about the requirements of each method, see Appendix B.1.

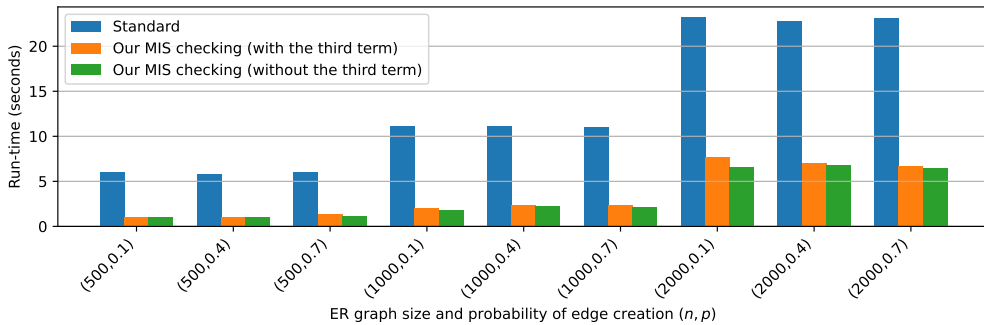


Figure 4: Run-time results of our MIS checking vs. the standard iterative approach across different graph sizes and densities.

- All learning-based methods, except for GCN, require training a separate network for each graph dataset, as indicated in the third and sixth columns of Table 1. This illustrates the generalization limitations of these methods. In contrast, our method is more generalizable, as it only requires tuning hyper-parameters for each set of graphs.
- Other than SATLIB DIFUSCO results, when compared to learning-based approaches, our method outperforms all baseline methods in terms of MIS size, all without requiring any training data. We note that the run-time reported for learning-based methods exclude training time, which may vary depending on multiple factors such as graph size, available compute, number of data points, and the used neural network architecture. For ER, in under 6 minutes (which is less than the inference time of any learning-based method), pCQO-MIS-1 and pCQO-MIS-2 report larger MIS sizes when compared to learning methods. Furthermore, our approach does not rely on additional techniques such as Greedy Decoding [36] and Monte Carlo Tree Search [37].
- When compared to iSCO, our method reports larger MIS sizes while requiring significantly reduced sequential run-time. We note that the iSCO paper [27] reports a lower run time as com-

pared to other methods. This reported run time is achieved by evaluating the test graphs in parallel, in contrast to all other methods that evaluated them sequentially. To fairly compare methods in our experiments, we opted to report sequential test run time only. We conjecture that the extended sequential run-time of iSCO, compared to its parallel run-time, is due to its use of simulated annealing. Because simulated annealing depends on knowing the energy of the previous step when determining the next step, it is inherently more efficient for iSCO to solve many graphs in parallel than in series.

- For SATLIB, which consists of highly sparse graphs, on average, pCQO-MIS falls short by a few nodes when compared to ReduMIS, Gurobi, and CP-SAT. The reason ReduMIS achieves SOTA results here is that a large set of MIS-specific graph reductions can be applied as well as applying the 2-opt local search [35] for multiple rounds. pCQO-MIS and other baselines do not apply the 2-opt procedure following the study in [20] where it was conjectured that most methods will converge to the same solutions if this local search procedure is applied. We note that ReduMIS iteratively applies this heuristic. For denser graphs, most of these graph reductions are not applicable. Gurobi (and CP-SAT) solves the ILP in (1) by which the number of constraints is equal to the number of edges in the graph. This means that Gurobi and CP-SAT are expected to perform much better in sparse graph such as SATLIB.
- On ER, our method not only reports a larger average MIS size but generally also requires less the run-time. Specifically, in 40.1 minutes, our method achieves better results than ReduMIS, CP-SAT, and Gurobi. In under 64 minutes, we achieve a new record for the obtained average MIS size which is 45. We emphasize that we outperform the SOTA MIS heuristic solver and two commercialized solvers⁵.
- Given the same run-time, when comparing the results of pQO-MIS (i.e., $\gamma' = 0$) and the results of pCQQ-MIS, we observe that when the MC term is included, pCQO-MIS reports larger MIS sizes. Specifically, on average, using the MC term yields nearly 9 (resp. 4) nodes improvement for SATLIB (resp. ER).
- We achieve competitive results using both pCQQ-MIS-1 pCQQ-MIS-2. However, restarting with the best optimized vector from a previous batch (i.e., pCQQ-MIS-2) is more beneficial for the SATLIB results.

4.3. Scalability Results

It is well-established that relatively denser graphs pose greater computational challenges compared to sparse graphs. This observation diverges from the trends exhibited by other non-data-centric baselines, which predominantly excel on sparse graphs. We argue that this is due to the applicability of graph reduction techniques such as the LP reduction method in [21], and the unconfined vertices rule [38] (see [13] for a complete list of the graph reduction rules that apply only on sparse graphs). For instance, by simply applying the LP graph reduction technique, the large-scale highly sparse graphs (with several hundred thousand nodes), considered in Table 5 of [31], reduce to graphs of a few thousands nodes with often dis-connected sub-graphs that can be treated independently.

Therefore, the scalability and performance of ReduMIS are significantly dependent on the sparsity of the graph. This dependence emerges from the iterative application of various graph reduction techniques (and the 2-opt local search in [35]) in ReduMIS, specifically tailored for sparse graphs. For instance, the ReduMIS results presented in Table 2 of [30] are exclusively based on very large and highly sparse graphs. This conclusion is substantiated by both the sizes of the considered graphs and the corresponding sizes of the obtained MIS solutions. As such, in this subsection, we investigate the scalability of pCQO-MIS for the MIS problem against the SOTA methods: ReduMIS, Gurobi, and CP-SAT. Here, we use randomly generated graphs with the GNM generator by which the number of edges is set to $m = \lceil \frac{n(n-1)}{4} \rceil$. It is important to note that the density of these graphs is significantly higher than those considered in the previous subsection (and most of previous works).

⁵We note that learning-based methods, such as [28, 29] use ReduMIS to label their training graphs under the supervised learning setting)

This choice of the number of edges in the GNM function indicate that half of the total possible edges (w.r.t. the complete graph) exist.

Results are provided in Figure 3. As observed, for dense graphs, as the graph size increases, our method requires significantly less run-time (Figure 3a) compared to all baselines, while reporting the same average MIS size (Table 3b). For instance, when n is 500, on average, our method requires around 15 minute to solve the 5 graphs, whereas other baselines require approximately 35 minutes or more to achieve the same MIS size. For the case of $n = 1500$, our method requires nearly 35 minutes whereas ReduMIS requires 244 minutes. These results indicate that, unlike ReduMIS and ILP solvers, the run-time of our method scales only with the number of nodes in the graph, which is a significant improvement.

4.4. Impact of the Proposed MIS Checking Criterion

In this subsection, we evaluate the impact of the proposed MIS checking method on the run-time performance of the pCQO-MIS algorithm. Specifically, we execute pCQO-MIS for $T = 1000$ iterations, performing MIS checking at each iteration. The results for 10 ER graphs, covering various graph sizes and densities, are illustrated in Figure 4, with the x-axis representing different graph sizes and densities. We compare these results to the standard MIS checking approach, which involves iterating over all nodes to examine their neighbors, as detailed in Section 3.3.3.

The results suggest that the execution time for pCQO-MIS is reduced with our efficient implementation compared to the standard method, across various graph sizes.

5. Conclusion

This study addressed the challenging Maximum Independent Set (MIS) Problem within the domain of Combinatorial Optimization by introducing a clique-Informed continuous quadratic formulation. By eliminating the need for any training data, pCQO-MIS sets itself apart from conventional learning approaches. Through the utilization of gradient-based optimization using Adam and a parallel GPU implementation, our straightforward yet effective approach demonstrates competitive performance compared to state-of-the-art learning-based and sampling-based methods. This research offers a distinctive perspective on approaching discrete optimization problems through parameter-efficient procedure that are optimized from the problem structure, not from datasets.

References

- [1] Richard M Karp. Reducibility among combinatorial problems. In *Complexity of computer computations*, pages 85–103. Springer, 1972.
- [2] Duncan C McElfresh, Hoda Bidkhori, and John P Dickerson. Scalable robust kidney exchange. In *Proceedings of the AAAI Conference on Artificial Intelligence*, volume 33, pages 1077–1084, 2019.
- [3] George B. Dantzig, Delbert R. Fulkerson, and Selmer M. Johnson. Solution of a large-scale traveling-salesman problem. *Journal of the Operations Research Society of America*, 2(4):393–410, 1954.
- [4] S. Matsui and K. Tokoro. A new genetic algorithm for minimum span frequency assignment using permutation and clique. In *Central Research Institute of Electric Power Industry*, Tokyo, Japan, 2000.
- [5] Duncan Eddy and Mykel J. Kochenderfer. A maximum independent set method for scheduling earth-observing satellite constellations. *Journal of Spacecraft and Rockets*, 58(5):1416–1429, 2021. doi: 10.2514/1.a34931.
- [6] Deborah Joseph, Joao Meidanis, and Prasoon Tiwari. Determining dna sequence similarity using maximum independent set algorithms for interval graphs. In *Algorithm Theory — SWAT*

- '92, volume 621 of *Lecture Notes in Computer Science*, pages 326–337. Springer, Berlin, Heidelberg, 1992. doi: 10.1007/3-540-55706-7_29.
- [7] Jules Roux, David Walshaw, and Sandeep Swain. Maximal clique and maximum independent set for genome assembly: Algorithms and applications. *Journal of Computational Biology*, 20(4): 123–136, 2023.
- [8] First Author and Second Author. Solving multi-robot coordination problems using maximum independent set techniques. *Journal of Robotics Research*, 45(3):123–135, 2024. doi: 10.1234/jrr.2024.01234. URL <https://www.example.com/your-article-link>.
- [9] Robert Endre Tarjan and Anthony E Trojanowski. Finding a maximum independent set. *SIAM Journal on Computing*, 6(3):537–546, 1977.
- [10] IBM. IBM ILOG CPLEX Optimization Studio. URL <https://www.ibm.com/products/ilog-cplex-optimization-studio>.
- [11] Gurobi. Gurobi Optimization. URL <https://www.gurobi.com>.
- [12] Google, Inc. Google or-tools. 2022. URL <https://developers.google.com/optimization>.
- [13] Sebastian Lamm, Peter Sanders, Christian Schulz, Darren Strash, and Renato F Werneck. Finding near-optimal independent sets at scale. In *2016 Proceedings of the Eighteenth Workshop on Algorithm Engineering and Experiments (ALENEX)*, pages 138–150. SIAM, 2016.
- [14] Takuya Akiba and Yoichi Iwata. Branch-and-reduce exponential/fpt algorithms in practice: A case study of vertex cover. *Theoretical Computer Science*, 609:211–225, 2016.
- [15] Pablo San Segundo, Diego Rodríguez-Losada, and Agustín Jiménez. An exact bit-parallel algorithm for the maximum clique problem. *Computers & Operations Research*, 38(2):571–581, 2011.
- [16] Ravi Boppana and Magnús M Halldórsson. Approximating maximum independent sets by excluding subgraphs. *BIT Numerical Mathematics*, 32(2):180–196, 1992.
- [17] Yoshua Bengio, Andrea Lodi, and Antoine Prouvost. Machine learning for combinatorial optimization: a methodological tour d’horizon. *European Journal of Operational Research*, 290(2): 405–421, 2021.
- [18] Ismail R Alkhouri, George K Atia, and Alvaro Velasquez. A differentiable approach to the maximum independent set problem using dataless neural networks. *Neural Networks*, 155: 168–176, 2022.
- [19] Martin JA Schuetz, J Kyle Brubaker, and Helmut G Katzgraber. Combinatorial optimization with physics-inspired graph neural networks. *Nature Machine Intelligence*, 4(4):367–377, 2022.
- [20] Maximilian Böther, Otto Kißig, Martin Taraz, Sarel Cohen, Karen Seidel, and Tobias Friedrich. What’s wrong with deep learning in tree search for combinatorial optimization. *arXiv preprint arXiv:2201.10494*, 2022.
- [21] George L Nemhauser and Leslie Earl Trotter. Vertex packings: Structural properties and algorithms. *Mathematical Programming*, 8(1):232–248, 1975.
- [22] Panos M Pardalos and Gregory P Rodgers. A branch and bound algorithm for the maximum clique problem. *Computers & operations research*, 19(5):363–375, 1992.
- [23] Foad Mahdavi Pajouh, Balabhaskar Balasundaram, and Oleg A Prokopyev. On characterization of maximal independent sets via quadratic optimization. *Journal of Heuristics*, 19:629–644, 2013.

- [24] Victor K Wei. A lower bound on the stability number of a simple graph. Technical report, Bell Laboratories Technical Memorandum Murray Hill, NJ, USA, 1981.
- [25] Samuel Burer and Adam N Letchford. On nonconvex quadratic programming with box constraints. *SIAM Journal on Optimization*, 20(2):1073–1089, 2009.
- [26] Aric A. Hagberg, Daniel A. Schult, and Pieter J. Swart. Exploring network structure, dynamics, and function using networkx. In Gaël Varoquaux, Travis Vaught, and Jarrod Millman, editors, *Proceedings of the 7th Python in Science Conference*, pages 11 – 15, Pasadena, CA USA, 2008.
- [27] Haoran Sun, Katayoon Goshvadi, Azade Nova, Dale Schuurmans, and Hanjun Dai. Revisiting sampling for combinatorial optimization. In *International Conference on Machine Learning*, pages 32859–32874. PMLR, 2023.
- [28] Ruizhong Qiu, Zhiqing Sun, and Yiming Yang. Dimes: A differentiable meta solver for combinatorial optimization problems. *Advances in Neural Information Processing Systems*, 35:25531–25546, 2022.
- [29] Zhiqing Sun and Yiming Yang. Difusco: Graph-based diffusion solvers for combinatorial optimization. *arXiv preprint arXiv:2302.08224*, 2023.
- [30] Sungsoo Ahn, Younggyo Seo, and Jinwoo Shin. Learning what to defer for maximum independent sets. In *International Conference on Machine Learning*, pages 134–144. PMLR, 2020.
- [31] Zhuwen Li, Qifeng Chen, and Vladlen Koltun. Combinatorial optimization with graph convolutional networks and guided tree search. In *NeurIPS*, 2018.
- [32] Paul Erdos, Alfréd Rényi, et al. On the evolution of random graphs. *Publ. Math. Inst. Hung. Acad. Sci*, 5(1):17–60, 1960.
- [33] Holger H Hoos and Thomas Stützle. Satlib: An online resource for research on sat. *Sat*, 2000: 283–292, 2000.
- [34] Sungsoo Ahn, Younggyo Seo, and Jinwoo Shin. Learning what to defer for maximum independent sets. In Hal Daumé III and Aarti Singh, editors, *Proceedings of the 37th International Conference on Machine Learning*, volume 119 of *Proceedings of Machine Learning Research*, pages 134–144. PMLR, 13–18 Jul 2020. URL <https://proceedings.mlr.press/v119/ahn20a.html>.
- [35] Diogo V Andrade, Mauricio GC Resende, and Renato F Werneck. Fast local search for the maximum independent set problem. *Journal of Heuristics*, 18(4):525–547, 2012.
- [36] Alexandros Graikos, Nikolay Malkin, Nebojsa Jojic, and Dimitris Samaras. Diffusion models as plug-and-play priors. *Advances in Neural Information Processing Systems*, 35:14715–14728, 2022.
- [37] Zhang-Hua Fu, Kai-Bin Qiu, and Hongyuan Zha. Generalize a small pre-trained model to arbitrarily large tsp instances. In *Proceedings of the AAAI conference on artificial intelligence*, volume 35, pages 7474–7482, 2021.
- [38] Mingyu Xiao and Hiroshi Nagamochi. Confining sets and avoiding bottleneck cases: A simple maximum independent set algorithm in degree-3 graphs. *Theoretical Computer Science*, 469:92–104, 2013.
- [39] Hanjun Dai, Bo Dai, and Le Song. Discriminative embeddings of latent variable models for structured data. In *International conference on machine learning*, pages 2702–2711. PMLR, 2016.
- [40] David P Williamson and David B Shmoys. *The design of approximation algorithms*. Cambridge university press, 2011.
- [41] Piotr Berman and Georg Schnitger. On the complexity of approximating the independent set problem. *Information and Computation*, 96(1):77–94, 1992.

- [42] Michaël Defferrard, Xavier Bresson, and Pierre Vandergheynst. Convolutional neural networks on graphs with fast localized spectral filtering. *Advances in neural information processing systems*, 29:3844–3852, 2016.
- [43] Jonathan Ho, Ajay Jain, and Pieter Abbeel. Denoising diffusion probabilistic models. *Advances in neural information processing systems*, 33:6840–6851, 2020.
- [44] Hanjun Dai, Elias B Khalil, Yuyu Zhang, Bistra Dilkina, and Le Song. Learning combinatorial optimization algorithms over graphs. In *Proceedings of the 31st International Conference on Neural Information Processing Systems*, pages 6351–6361, 2017.
- [45] John Schulman, Filip Wolski, Prafulla Dhariwal, Alec Radford, and Oleg Klimov. Proximal policy optimization algorithms. *arXiv preprint arXiv:1707.06347*, 2017.
- [46] Yuma Ichikawa. Controlling continuous relaxation for combinatorial optimization. *arXiv preprint arXiv:2309.16965*, 2023.
- [47] Katayoon Goshvadi, Haoran Sun, Xingchao Liu, Azade Nova, Ruqi Zhang, Will Grathwohl, Dale Schuurmans, and Hanjun Dai. Discs: A benchmark for discrete sampling. *Advances in Neural Information Processing Systems*, 36, 2024.
- [48] Haoran Sun, Hanjun Dai, Wei Xia, and Arun Ramamurthy. Path auxiliary proposal for mcmc in discrete space. In *International Conference on Learning Representations*, 2021.

Appendix

A. Proofs

We begin by re-stating our main optimization problem:

$$\min_{\mathbf{x} \in [0,1]^n} f(\mathbf{x}) := - \sum_{v \in V} \mathbf{x}_v + \gamma \sum_{(u,v) \in E} \mathbf{x}_v \mathbf{x}_u - \gamma' \sum_{(u,v) \in E'} \mathbf{x}_v \mathbf{x}_u = -\mathbf{e}_n^T \mathbf{x} + \frac{\gamma}{2} \mathbf{x}^T \mathbf{A}_G \mathbf{x} - \frac{\gamma'}{2} \mathbf{x}^T \mathbf{A}_{G'} \mathbf{x}. \quad (12)$$

The gradient of (12) is:

$$\nabla_{\mathbf{x}} f(\mathbf{x}) = -\mathbf{e}_n + (\gamma \mathbf{A}_G - \gamma' \mathbf{A}_{G'}) \mathbf{x}. \quad (13)$$

For some $v \in V$, we have

$$\frac{\partial f(\mathbf{x})}{\partial \mathbf{x}_v} = -1 + \gamma \sum_{u \in \mathcal{N}(v)} \mathbf{x}_u - \gamma' \sum_{u \in \mathcal{N}'(v)} \mathbf{x}_u \quad (14)$$

A.1. Proof of Lemma 1

Re-statement: For any non-complete graph G , the constant hessian of $f(\mathbf{x})$ in (12) is always a non-PSD matrix.

Proof. From (12), the hessian is $(\gamma \mathbf{A}_G - \gamma' \mathbf{A}_{G'})$ and is independent of \mathbf{x} . If $(\gamma \mathbf{A}_G - \gamma' \mathbf{A}_{G'})$ is PSD, then, by definition of PSD matrices, we must have

$$\mathbf{x}^T (\gamma \mathbf{A}_G - \gamma' \mathbf{A}_{G'}) \mathbf{x} \geq 0, \forall \mathbf{x} \in [0, 1]^n, \quad (15)$$

which is not possible as for any \mathbf{x}_0 that corresponds to an MIS, we have $\mathbf{x}_0^T (\gamma \mathbf{A}_G) \mathbf{x}_0 = 0$ (no edges in MIS w.r.t. G) and $\gamma' \mathbf{x}_0^T \mathbf{A}_{G'} \mathbf{x}_0 < 0$ (a MIS in G is a clique in G'). \square

A.2. Proof of Theorem 1

Re-statement: Given an arbitrary graph $G = (V, E)$ and its corresponding formulation in (12), suppose the size of the largest MIS of G is k . Then, $\gamma \geq \gamma' k + 1$ is necessary and sufficient for all MIS vectors to be local minimizers of (12) for arbitrary graphs.

Proof. Let \mathcal{I} be an MIS. Define the vector $\mathbf{x}^{\mathcal{I}}$ such that it contains 1's at positions corresponding to the nodes in the set S , and 0's at all other positions. For any MIS to be a local minimizer of (12), it is sufficient and necessary to require that

$$\frac{\partial f(\mathbf{x})}{\partial \mathbf{x}_v} \geq 0, \quad \forall v \notin \mathcal{I} \text{ and} \quad (16)$$

$$\frac{\partial f(\mathbf{x})}{\partial \mathbf{x}_v} \leq 0, \quad \forall v \in \mathcal{I}. \quad (17)$$

Here, \mathbf{x}_v is the element of \mathbf{x} at the position corresponding to the node v . (16) is derived because if $v \notin \mathcal{I}$, then $\mathbf{x}_v^{\mathcal{I}} = 0$ (by the definition of $\mathbf{x}^{\mathcal{I}}$) so it is at the left boundary of the interval $[0, 1]$. For the left boundary point to be a local minimizer, it requires the derivative to be non-negative (i.e., moving towards the right only increases the objective). Similarly, when $v \in \mathcal{I}$, $\mathbf{x}_v^{\mathcal{I}} = 1$, is at the right boundary for (17), at which the derivative should be non-positive.

The derivative of f computed in (14) can be rewritten as

$$\frac{\partial f(\mathbf{x})}{\partial \mathbf{x}_v} = -1 + \gamma m_v - \gamma' \ell_v, \quad \forall v \notin \mathcal{I}, \quad (18)$$

where $m_v := |\{u \in \mathcal{N}(v) \cap \mathcal{I}\}|$ is the number of neighbours of v in \mathcal{I} and ℓ_v is the number of non-neighbours of v in \mathcal{I} i.e., $\ell_v := |\{u \in \mathcal{N}'(v) \cap \mathcal{I}\}|$ where $\mathcal{N}'(v) = \{u : (u, v) \in E'\}$. By this definition, we immediately have $1 \leq m_v \leq |\mathcal{I}|$ and $0 \leq \ell_v \leq |\mathcal{I}|$, where the upper and lower bounds for m_v and ℓ_v are all attainable by some special graphs. Note that the lower bound of m_v is 1, and that is due the fact that \mathcal{I} is a MIS, so any other node (say v) will have at least 1 edge connected to a node in \mathcal{I} .

Plugging (18) into (16), we obtain

$$\gamma \geq \frac{1 + \gamma' \ell_v}{m_v} \quad (19)$$

Since we're seeking a universal γ for all the graphs, we must set m_v to its lowest possible value, 1, and ℓ_v to its highest possible value k (both are attainable by some graphs), and still requires γ to satisfy (19). This means it is necessary and sufficient to require $\gamma \geq \gamma'k + 1$. In addition, (17) is satisfied unconditionally and therefore does not impose any extra condition on γ . \square

A.3. Proof of Lemma 2

Re-statement: All local minimizers of (12) are binary vectors.

Proof. Let \mathbf{x}^* be any local minimizer of (12), if all the coordinates of \mathbf{x}^* are either 0 or 1, then \mathbf{x}^* is binary and the proof is complete, otherwise, at least one coordinate of \mathbf{x}^* is in the interior $(0, 1)$ and we aim to prove that this is not possible (i.e. such a non-binary \mathbf{x}^* cannot exist as a minimizer) by contradiction. We assume the non-binary \mathbf{x}^* exists, and denote the set of non-binary coordinates as

$$J := \{j : \mathbf{x}_j^* \in (0, 1)\}. \quad (20)$$

Since \mathbf{x}^* is non-binary, $J \neq \emptyset$. Since the objective function $f(\mathbf{x})$ of (12) is twice differentiable with respect to all \mathbf{x}_j with $\mathbf{x}_j \in (0, 1)$, then a necessary condition for \mathbf{x}^* to be a local minimizer is that

$$\nabla f(\mathbf{x}^*)|_J = 0, \quad \nabla^2 f(\mathbf{x}^*)|_J \succeq 0,$$

where $\nabla f(\mathbf{x}^*)|_J$ is the vector $\nabla f(\mathbf{x}^*)$ restricted to the index set J , and $\nabla^2 f(\mathbf{x}^*)|_J$ is the matrix $\nabla^2 f(\mathbf{x}^*)$ whose row and column indices are both restricted to the set J .

However, the second necessary condition $\nabla^2 f(\mathbf{x}^*)|_J \succeq 0$ cannot hold. Because if it does, then we must have $\text{tr}(\nabla^2 f(\mathbf{x}^*)|_J) > 0$ (the trace cannot strictly equal to 0 as $\nabla^2 f(\mathbf{x}^*)|_J = \mathbf{I}_J(\gamma \mathbf{A}_G - \gamma' \mathbf{A}_{G'}) \mathbf{I}_J^T \neq 0$). However, on the other hand, we have

$$\text{tr}(\nabla^2 f(\mathbf{x}^*)|_J) = \text{tr}(\mathbf{I}_J(\gamma \mathbf{A}_G - \gamma' \mathbf{A}_{G'}) \mathbf{I}_J^T) = 0$$

as the diagonal entries of \mathbf{A}_G and $\mathbf{A}_{G'}$ are all 0, which leads to a contradiction. Here \mathbf{I}_J denotes the identity matrix with row indices restricted to the index set J . \square

A.4. Proof of Theorem 2

Re-statement: Given graph $G = (V, E)$ and set $\gamma \geq 1 + \gamma' \Delta(G')$, all local minimizers of (12) correspond to an MIS in G .

Proof. By lemma 2, we can only consider binary vectors as local minimizers. With this, we first prove that all local minimizers are Independent Sets (ISs). Then, we show that any IS, that is not a maximal IS, is not a local minimizer.

Here, we show that any local minimizer is an IS. By contradiction, assume that vector \mathbf{x} , by which $\mathbf{x}_v = \mathbf{x}_w = 1$ such that $(v, w) \in E$ (a binary vector with an edge in G), is a local minimizer. Since $\mathbf{x}_v = 1$ is at the right boundary of the interval $[0, 1]$, for it to be a local minimizer, we must have $\frac{\partial f}{\partial \mathbf{x}_v} \leq 0$. Together with (14), this implies

$$-1 + \gamma \sum_{u \in \mathcal{N}(v)} \mathbf{x}_u - \gamma' \sum_{u \in \mathcal{N}'(v)} \mathbf{x}_u \leq 0. \quad (21)$$

Re-arranging (21) and using $\gamma \geq n$ yields to

$$\gamma \sum_{u \in \mathcal{N}(v)} \mathbf{x}_u \leq 1 + \gamma' \sum_{u \in \mathcal{N}'(v)} \mathbf{x}_u. \quad (22)$$

Given that $\gamma \geq 1 + \gamma' \Delta(G')$, the condition in (22) can not be satisfied even if the LHS attains its minimum value (which is γn) and the RHS attains a maximum value. The maximum possible value of the RHS is $1 + d'(v) = n - d(v)$, where $d'(v)$ is the degree of node v in G' , and the maximum possible value of $d'(v)$ is $\Delta(G')$. This means that when an edge exists in \mathbf{x} , it can not be a fixed point. Thus, only ISs are local minimizers.

Here, we show that Independent Sets that are not maximal are not local minimizers. Define vector $\mathbf{x} \in \{0, 1\}^n$ that corresponds to an IS $\mathcal{I}(\mathbf{x})$. This means that there exists a node $u \in V$ that is not in the IS and is not in the neighbor set of all nodes in the IS. Formally, if there exists $u \notin \mathcal{I}(\mathbf{x})$ such that $\forall w \in \mathcal{I}(\mathbf{x}), u \notin \mathcal{N}(w)$, then $\mathcal{I}(\mathbf{x})$ is an IS, not a maximal IS. Note that such an \mathbf{x} satisfies $\mathbf{x}_u = 0$ and

$$\frac{\partial f}{\partial \mathbf{x}_u} = -1 + \gamma \sum_{u \in \mathcal{N}(v)} \mathbf{x}_u - \gamma' \sum_{u \in \mathcal{N}'(v)} \mathbf{x}_u = -1 - \gamma' \sum_{u \in \mathcal{N}'(v)} \mathbf{x}_u < 0, \quad (23)$$

which implies increasing \mathbf{x}_u can further decrease the function value, contradicting to \mathbf{x} being a local minimizer. In (23), the second summation is 0 as $\mathcal{N}(v) \cap \mathcal{I}(\mathbf{x}) = \emptyset$, which results in $-(1 + \gamma' \sum_{u \in \mathcal{N}'(v)} \mathbf{x}_u)$ that is always negative. Thus, any binary vector that corresponds to an IS that is not maximal is not a local minimizer. \square

A.5. Proof of Theorem 3

Re-statement: For any graph G , assume that there exists a point \mathbf{x}' such that $\nabla_{\mathbf{x}} f(\mathbf{x}') = \mathbf{0}$, i.e., $\mathbf{x}' = (\gamma \mathbf{A}_G - \gamma' \mathbf{A}_{G'})^{-1} \mathbf{e}_n$. Then \mathbf{x}' is not a local minimizer of (12) and therefore does not correspond to a MIS.

Proof. By Lemma 2, we know that all local minimizers are binary. By contradiction, assume that \mathbf{x}' is a binary local minimizer. Then, the system of equations $(\gamma \mathbf{A}_G - \gamma' \mathbf{A}_{G'}) \mathbf{x}' = \mathbf{e}_n$ implies that, for all $v \in V$, the following equality must be satisfied.

$$\gamma \sum_{u \in \mathcal{N}(v)} \mathbf{x}'_u - \gamma' \sum_{u \in \mathcal{N}'(v)} \mathbf{x}'_u = 1. \quad (24)$$

If \mathbf{x}' is binary and corresponds to a MIS in the graph, then the first term of (24) is always 0, which reduces (24) to

$$-\gamma' \sum_{u \in \mathcal{N}'(v)} \mathbf{x}'_u = 1. \quad (25)$$

Eq.(25) is an equality that can not be satisfied as $\mathbf{x}'_v \geq 0, \forall v \in V$ and $\gamma' \geq 1$. Thus, \mathbf{x}' is not a local minimizer. \square

B. Related work

1) Exact and Heuristic Solvers: Exact approaches for NP-hard problems typically rely on branch-and-bound global optimization techniques. However, exact approaches suffer from poor scalability, which limits their uses in large MIS problems [39]. This limitation has spurred the development of efficient approximation algorithms and heuristics. For instance, the well-known NetworkX library [26] implements a heuristic procedure for solving the MIS problem [16]. These polynomial-time heuristics often incorporate a mix of sub-procedures, including greedy algorithms, local search sub-routines, and genetic algorithms [40]. However, such heuristics generally cannot theoretically guarantee that the resulting solution is within a small factor of optimality. In fact, inapproximability results have been established for the MIS [41].

Among existing MIS heuristics, ReduMIS [13] has emerged as the leading approach. The ReduMIS framework contains two primary components: (i) an iterative application of various graph reduction techniques (e.g., the linear programming (LP) reduction method in [21]) with a stopping rule based on the non-applicability of these techniques; and (ii) an evolutionary algorithm. The ReduMIS algorithm initiates with a pool of independent sets and evolves them through multiple rounds. In each round, a selection procedure identifies favorable nodes by executing graph partitioning, which clusters the graph nodes into disjoint clusters and separators to enhance the solution. In contrast, our pCQO-MIS approach does *not* require such complex algorithmic operations (e.g., solution combination operation, community detection, and local search algorithms for solution improvement) as used in ReduMIS. More importantly, ReduMIS and ILP solvers scale with the number of nodes and the number of edges (which constraints their application on highly dense graphs), whereas pCQO-MIS only scales w.r.t. the number nodes, as will be demonstrated in our experimental results.

2) Data-Driven Learning-Based Solvers: Data-driven approaches for MIS problems can be classified into SL and RL methods. These methods depend on neural networks trained to for the distribution over (un)labeled training graphs.

A notable SL method is proposed in [31], which combines several components including graph reductions [13], Graph Convolutional Networks (GCN) [42], guided tree search, and a solution improvement local search algorithm [35]. The GCN is trained on benchmark graphs using their solutions as ground truth labels, enabling the learning of probability maps for the inclusion of each vertex in the optimal solution. Then, a subset of ReduMIS subroutines is used to improve their solution. While the work in [31] reported on-par results to ReduMIS, it was later shown by [20] that replacing the GCN output with random values performs similarly to using the trained GCN network. Recently, DIFUSCO was introduced in [29], an approach that integrates Graph Neural Networks (GNNs) with diffusion models [43] to create a graph-based diffusion denoiser. DIFUSCO formulates the MIS problem in the discrete domain and trains a diffusion model to improve a single or a pool of solutions.

On the other hand, RL-based methods have achieved more success in solving the MIS problem when compared to SL methods. In the work of [44], a Deep Q-Network (DQN) is combined with graph embeddings, facilitating the discrimination of vertices based on their influence on the solution and ensuring scalability to larger instances. Meanwhile, the study presented in [30] introduces the Learning What to Defer (LwD) method, an unsupervised deep RL solver resembling tree search, where vertices are iteratively assigned to the independent set. Their model is trained using Proximal Policy Optimization (PPO) [45]. The work in [28] introduces DIMES, which combines a compact continuous space to parameterize the distribution of potential solutions and a meta-learning framework to facilitate the effective initialization of model parameters during the fine-tuning stage that is required for each graph.

It is worth noting that the majority of SL and RL methods are *data-dependent* in the sense that they require the training of a separate network for each dataset of graphs. These data-dependent methods exhibit limited *generalization* performance when applied to out-of-distribution graph data. This weak generalization stems from the need to train a different network for each graph dataset. In contrast, our dQNN approach differs from SL- and RL-based methods in that it does not rely on any training datasets. Instead, our dQNN approach utilizes a simple yet effective *graph-encoded* continuous objective function, which is defined solely in terms of the connectivity of a given graph.

3) Dataless Differentiable Methods: The method in [18] introduced dataless neural networks (dNNs) tailored for the MIS problem. Notably, their method operates without the need for training data and relies on n trainable parameters. Their proposed methodology advocates using a ReLU-based continuous objective to solve the MIS problem. However, to scale up and improve their method, graph partitioning and local search algorithms were employed. The method in [46] introduced a method that optimizes the parameters of a NN over one graph.

4) **Discrete Sampling Solvers:** In recent studies, researchers have explored the integration of energy-based models with parallel implementations of simulated annealing to address combinatorial optimization problems [47] without relying on any training data. For example, in tackling the Maximum Independent Set (MIS) problem, Sun et al. [27] proposed a solver that combines (i) Path Auxiliary Sampling [48] and (ii) the binary quadratic integer program in (2). However, unlike pCQO-MIS, these approaches entail prolonged sequential runtime and require fine-tuning of several hyperparameters. Moreover, the energy models utilized in this method for addressing the MIS problem may generate binary vectors that violate the “no edges” constraint inherent to the MIS problem. Consequently, a post-processing procedure becomes necessary.

B.1. Requirements Comparison with Baselines

In Table 2, we provide an overview comparison of the number of trainable parameters, hyperparameters, and additional techniques needed for each baseline. ReduMIS depends on a large set of graph reductions (see Section 3.1 in [13]) and graph clustering, which is used for solution improvement.

Table 2: Requirements comparison with baselines. For the ILPs (Gurobi and CP-SAT), trainable parameters correspond to n binary decision variables. ReduMIS is not an optimization method. However, they use n binary variables, one for each node.

Method	Size	Hyper-Parameters	Additional Techniques/Procedures
ReduMIS	n variables	N/A	Many graph reductions, and graph clustering
Gurobi	n variables	N/A	N/A
CP-SAT	n variables	N/A	N/A
GCN	$\gg n$ trainable parameters	Many as it is learning-based	Tree Search
LwD	$\gg n$ trainable parameters	Many as it is learning-based	Entropy Regularization
DIMES	$\gg n$ trainable parameters	Many as it is learning-based	Tree Search or Sampling Decoding
DIFUSCO	$\gg n$ trainable parameters	Many as it is learning-based	Greedy Decoding or Sampling Decoding
iSCO	n variables	Temperature, Sampler, Chain length	Post Processing for Correction
pCQO-MIS	n trainable parameters	Learning rate, exploration parameter η , number of steps T , momentum parameters β	Degree-based Initialization

For learning-based methods, although they attempt to ‘fit’ a distribution, the parameters of a neural network architecture are optimized during training. This architecture is typically much larger than the number of input coordinates ($\gg n$). For instance, the network used in DIFUSCO consists of 12 layers, each with 5 trainable weight matrices. Each weight matrix is 256×256 , resulting in 3932160 trainable parameters for the SATLIB dataset (which has at most 1347 nodes). Moreover, this dependence on training a NN introduces several hyper-parameters such as the number of layers, size of layers, choice of activation functions, etc.

It’s important to note that the choice of the sampler in iSCO introduces additional hyper-parameters. For instance, the PAS sampler [48] used in iSCO depends on the choice of the neighborhood function, a prior on the path length, and the choice of the probability of acceptance.

In terms of the number of optimization variables, pCQO-MIS only requires n variables and a much-reduced number of hyper-parameters compared to iSCO.

C. Additional Experiments

Table 3: Hyper-parameters for pCQO-MIS.

Graph Dataset	Edges-penalty γ	MC parameter γ'	Step size α	Momentum β	Optimization steps T	Exploration parameter η
SATLIB	900	1	3e-4	0.875	30	2.25
ER	350	7	9e-6	0.9	450	2.25

C.1. Comparison with the Relu-based Dataless Solver

Here, we compare pCQO-MIS with the dNN MIS solver in [18]. In this experiment, we use 10 GNM graphs with $(n, m) = (100, 500)$ and report the average MIS size and run-time (in seconds). The

results are given in Table 4. As observed, pCQO-MIS outperforms the dNN-MIS method in [18] in terms of both the run-time and MIS size.

Table 4: Evaluation of pCQO-MIS vs. the MIS dNN solver in [18] in terms of MIS size and run-time (seconds) over 10 GNM graphs with $(n, m) = (100, 500)$.

Method	Average MIS Size	Average Run-Time (seconds)
dNN-MIS [18]	27.4	24
pCQO-MIS-1 (Ours)	29.9	0.7

C.2. Comparison with Leading data-centric Solver with Different Densities

In this subsection, we compare our approach with the leading data-driven baseline, DIFUSCO. DIFUSCO uses a pre-trained diffusion model trained on ER700 graphs (with $p = 0.15$) labeled using ReduMIS, and is tested across graphs with varying edge creation probabilities, p . The results, presented in Table 5, are averaged over 32 graphs for each p , with DIFUSCO utilizing 4-sample decoding. For pCQO-MIS, hyperparameters remain fixed across all values of p .

Table 5: Evaluation of pCQO-MIS vs. the ER700-trained DIFUSCO (with $p = 0.15$) in [29] in terms of MIS size and run-time (minutes) averaged over 32 ER graphs for each p .

Probability of Edge Creation p	DIFUSCO MIS Size	DIFUSCO Run-Time	pCQO-MIS-1 MIS Size	pCQO-MIS-1 Run-Time
0.05	88.25	4.62	97.34	4.73
0.10	58	8.63	59.25	4.71
0.15 (The training setting of DIFUSCO)	40.81	12.98	43.2	4.67
0.2	29.22	17.66	33.78	4.45

As observed, our method consistently outperforms DIFUSCO in both average MIS size and run-time. Notably, our run-time remains constant as the number of edges increases, supporting our claim that the run-time scales only with the number of nodes in the graph. DIFUSCO reports relatively smaller MIS sizes, particularly for $p = 0.05$ and $p = 0.2$, which are slightly different from the training graphs. This underscores the generalization limitations of the leading learning-based method.

C.3. Empirical Observations on the non-Extremal Stationary Point \mathbf{x}'

In this section, we empirically demonstrate how the non-extremal stationary point \mathbf{x}' , analyzed in Theorem 3, varies with the type of graph. Specifically, we aim to show that, for many types of graphs, this saddle point is outside the box constraints, depending on the graph density. To this end, we consider GNM and ER graphs with different densities, as well as small and large graphs from the SATLIB dataset.

In Figure 5, we obtain $\mathbf{x}' = (\gamma \mathbf{A}_G - \gamma' \mathbf{A}_{G'})^{-1} \mathbf{e}_n$ with $\gamma = n$ and $\gamma' = 1$ for every considered graph. Each subplot in Figure 5 shows the values of \mathbf{x}'_v (y-axis) for every node $v \in V$ (x-axis), with the title specifies the graph used.

As observed, among all the graphs, only the very-high-density GNM graph (with results shown inside the dashed box in Figure 5) has $\mathbf{x}' \in [0, 1]^{100}$. Note that this graph was generated with $m = 4945$ where the total number of possible edges in the complete graph with $n = 100$ is 4950 edges. For all other graphs, we have $\mathbf{x}' \notin [0, 1]^n$, as indicated by the values strictly below 0. This means that, by applying the box-constraints projection, \mathbf{x}' is infeasible.

C.4. Sensitivity to the Edges-penalty Parameter γ

In Figure 6, we include results of our pCQO-MIS using different values of γ with learning rate of 0.6 and $\gamma' = 1$. We choose 10 ER graphs from the ER700 dataset. Subsequently, we use values between 50 and 800, following our theoretical results. As observed, we achieve very good results on all of

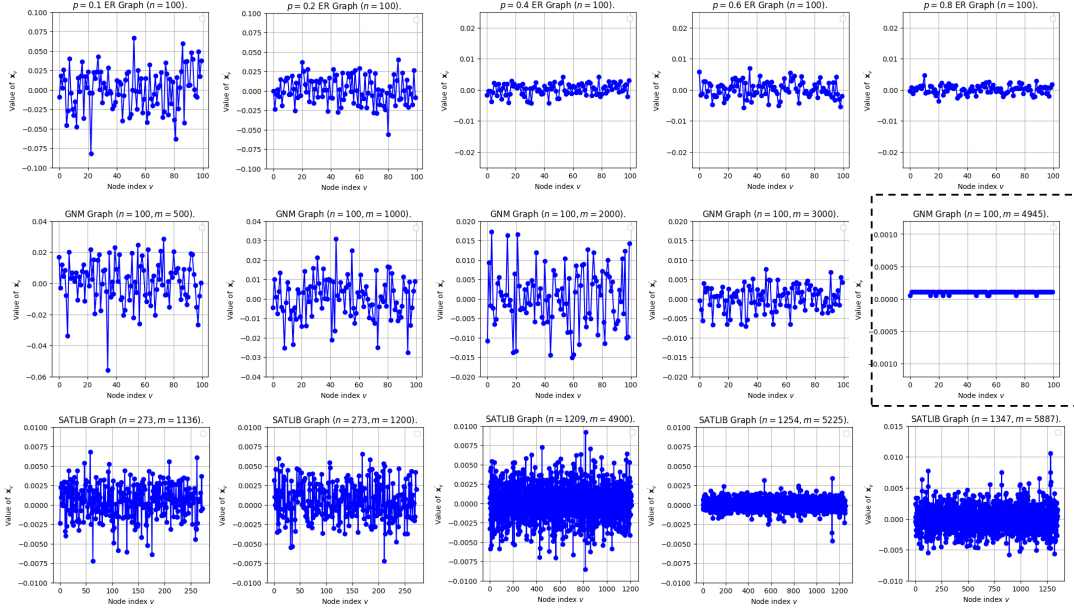


Figure 5: Values of the non-extremal stationary point \mathbf{x}' (y-axis) w.r.t. every node $v \in V$ (x-axis) across different ER and GNM graphs as well as small and large SATLIB graphs, as indicated by the title of each subplot. Among all the considered graphs, only the high-density GNM graph, indicated by the dashed square, has $\mathbf{x}' \in [0, 1]^{100}$.

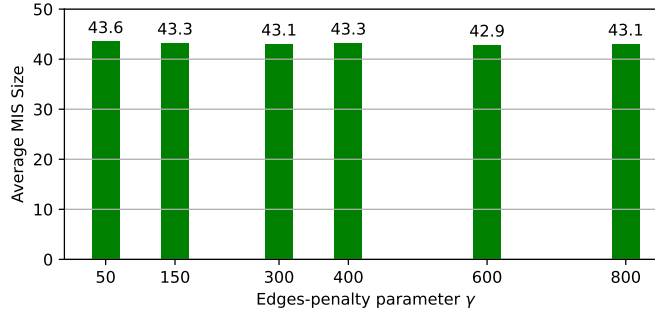


Figure 6: Evaluation of pCQO-MIS using different values of the edges-penalty parameter, γ . The results are averaged over 10 ER graphs from the ER700 dataset.

these values of the edges-penalty parameter, indicating that our method is not sensitive as long as the choice of follows our theorems.